

Constraints on kinematic parameters at $z \neq 0$

C. Rodrigues Filho^{1,2,*} and Edésio M. Barboza Jr.^{3,†}

¹*Universidade do Estado do Rio Grande do Norte,*

Departamento de Física, 59610-210, Mossoró - RN, Brasil

²*Universidade Federal do Rio Grande do Norte, Departamento de Física Teórica e Experimental, 59072-970, Natal-RN, Brasil*

³*Departamento de Física, Universidade do Estado do Rio Grande do Norte, 59610-210, Mossoró - RN, Brasil*

(Dated: April 27, 2017)

The standard cosmographic approach consists in performing a series expansion of a cosmological observable around $z = 0$ and then using the data to constrain the cosmographic (or kinematic) parameters at present time. Such a procedure works well if applied to redshift ranges inside the z -series convergence radius ($z < 1$), but can be problematic if we want to cover redshift intervals that fall outside the z -series convergence radius. This problem can be circumvented if we work with the y -redshift, $y = z/(1+z)$, or the scale factor, $a = 1/(1+z) = 1-y$, for example. In this paper, we use the scale factor a as the variable of expansion. We expand the luminosity distance and the Hubble parameter around an arbitrary \tilde{a} and use the Supernovae Ia (SNe Ia) and the Hubble parameter data to estimate H , q , j and s at $z \neq 0$ ($\tilde{a} \neq 1$). The results obtained from SNe Ia data are compatible with the Λ CDM model at 2σ confidence level. On the other hand, at 2σ confidence level, the results obtained from $H(z)$ data are incompatible with the Λ CDM model. These conflicting results may indicate a tension between the current SNe Ia and $H(z)$ data sets.

I. INTRODUCTION

By the end of 20th century it was discovered that the Universe is expanding at an accelerating rate [1, 2]. The current cosmic acceleration can be explained by the existence of a positive cosmological constant in the Einstein field equations [3]. However, the cosmological constant presents a huge discrepancy between its observed and its theoretical value [4]. Modifications of gravity theory [5–11] and exotic forms of fields [12–14] are some alternatives to the cosmological constant to explain the cosmic acceleration. However, the information about the cosmological parameters obtained from these alternative scenarios largely depends on the model under consideration.

Cosmokinetics (or cosmography) [15–20] is the least model-dependent method to get information about Universe expansion history. The basic assumption of cosmokinetics is the cosmological principle. No assumptions about sources or gravity theory are made. Therefore, it is expected that the results obtained from this kinematic approach remain valid regardless of the underlying cosmology. This feature may be an efficient weapon to probe the viability of several cosmological models proposed to describe the current phase of accelerated expansion of the Universe. For instance, since $j(z) = 1$ for the Λ CDM model, we can rule out this model if we find that $j \neq 1$.

Cosmography methodology consists of expanding cosmological observables such as the Hubble parameter and the luminosity distance in power series. However, to obtain some information about the kinematic state of the Universe, these series should be stopped. In such

an approximate process issues arise concerning the series convergence and the series truncation order. The series convergence problem can be circumvented by choosing a suitable expansion variable such as the so-called y -redshift, $y = z/(1+z)$ [21, 22], or the scale factor, $a = (1+z)^{-1} = 1-y$ [23], instead of the z redshift. The series truncation problem can be alleviated by performing the so-called F -test [21, 22, 24] to find which truncation order provides the more statistically significant fit to a given data set.

In this paper we follow the procedure adopted in [23] and perform the series expansion of the luminosity distance, $d_L(a)$, and of the Hubble parameter $H(a)$ around an arbitrary scale factor \tilde{a} . The F -test indicates that the most statistically significant truncation order for both series is the third. Since the third order approximation of d_L has one parameter less than the third order truncation of H , we include one more term in the d_L approximation to make the results obtained from these two series comparable. We use some of the most recent Type Ia Supernovae (SNe Ia) and $H(z)$ data sets to constrain the Hubble (H), deceleration (q), jerk (j) and snap (s) kinematic parameters at $z \neq 0$. At 2σ confidence level the results obtained from SNe Ia data are compatible with the Λ CDM model while the results obtained from $H(z)$ data are not compatible with this model. The constraints on j and s are conflicting and indicate a discrepancy between SNe Ia and $H(z)$ measurements.

II. COSMOKINETICS

Cosmokinetics relies on the assumption that at large scales the Universe is homogeneous and isotropic. Mathematically, this assumption is translated by the Robertson-Walker (RW) metric

*Electronic address: cornelio@fisica.ufrn.br

†Electronic address: edesio@barboza@uern.br

$$ds^2 = -c^2 dt^2 + a^2(t) \left[\frac{dr^2}{1 - kr^2} + r^2(d\theta^2 + \sin^2 \theta d\phi^2) \right], \quad (1)$$

where $a(t)$ is the scale factor of the Universe and k is the Universe spatial curvature. In agreement with recent results of the CMB power spectrum [25], we restrict our attention to a spatially flat Universe ($k = 0$) in this paper. For a flat RW line element, the luminosity distance takes the form,

$$d_L = c \frac{1}{a} \int_t^{t_0} \frac{dt'}{a(t')} = c(1+z) \int_0^z \frac{dz'}{H(z')}, \quad (2)$$

where the subscript 0 denotes the value of a variable at the present epoch, $H \equiv a^{-1}(da/dt)$ is the Hubble parameter, which provides the expansion rate of the Universe, and we have used the convention $a_0 = 1$.

Cosmokinetics works at time domains where a complete knowledge of the $a(t)$ function is not necessary. The standard approach consists in performing a Taylor expansion of a cosmological observable in terms of the redshift, keeping the expansion center fixed at $z = 0$ [15–17]. By focusing on the Hubble parameter and the luminosity distance, such a procedure leads to

$$\begin{aligned} H(z) = & H_0 \left[1 + (1 + q_0)z + \frac{1}{2}(j_0 - q_0^2)z^2 \right. \\ & + \frac{1}{6}(3q_0^3 + 3q_0^2 - 3j_0 + 4q_0j_0 - s_0)z^3 \\ & + \frac{1}{24}(l_0 + 8s_0 + 7q_0s_0 + 12j_0 + 32q_0j_0 + 25q_0^2j_0 \\ & \left. - 4j_0^2 - 12q_0^2 - 24q_0^3 - 15q_0^4)z^4 + \dots \right] \end{aligned} \quad (3)$$

and

$$\begin{aligned} d_L(z) = & \frac{c}{H_0} \left\{ z + \frac{1}{2}(1 - q_0)z^2 + \frac{1}{6}(3q_0^2 + q_0 - 1 - j_0)z^3 \right. \\ & + \frac{1}{24}(2 - 2q_0 - 15q_0^2 - 15q_0^3 + 5j_0 + 10q_0j_0 \\ & + s_0)z^4 - \frac{1}{120}[6(1 - q_0) - 3q_0^2(27 + 55q_0 - 35q_0^2) \\ & + 5q_0j_0(21q_0 + 22) + 15q_0s_0 - 10j_0^2 \\ & \left. + 27j_0 + 11s_0 + l_0]z^5 + \dots \right\}, \end{aligned} \quad (4)$$

where

$$q \equiv -\frac{\ddot{a}}{H^2 a}, \quad j \equiv \frac{\dddot{a}}{H^3 a}, \quad s \equiv \frac{\ddot{a}}{H^4 a} \quad \text{and} \quad l \equiv \frac{a^{(5)}}{H^5 a} \quad (5)$$

are, respectively, the deceleration, the jerk, the snap and the lerk parameters, and the dot denotes time derivatives. These parameters provide information about the kinematic state of the Universe. Physically, q specifies if the Universe is expanding at an accelerated ($q < 0$), decelerated ($q > 0$) or constant ($q = 0$) rate; j shows whether

the Universe's acceleration is increasing ($j > 0$), decreasing ($j < 0$) or constant ($j = 0$); s tells us if d^3a/dt^3 is increasing ($s > 0$), decreasing ($s < 0$) or constant ($s = 0$) and l tells us if d^4a/dt^4 is increasing ($l > 0$), decreasing ($l < 0$) or constant ($l = 0$). Thus, the kinematic approach allows us to investigate the cosmic acceleration without assuming modifications of the gravity theory or dark energy models.

The truncation of the expansions (3) and (4) at the first two or three terms should be good approximations if z does not lie outside the convergence radius of these series, $z < 1$ [21, 22]. However, currently we have measurements of H and d_L at $z > 1$. Applying low order approximations to cover such a redshift range may result in artificially strong constraints on the free parameters, while taking higher order terms, and consequently increasing the number of free parameters, can make the analysis more laborious than necessary. Therefore, we need to find a way to cover the higher redshift range using the lowest number of parameters possible. This problem can be handled if we work with the y -redshift, $y = z/(1+z)$ [21, 22] which maps the redshift domain $z \in [0, \infty[$ into $y \in [0, 1[$ or, equivalently, if we work with the scale factor a ($a = 1 - y$) [23] as expansion variables. Here we choose the scale factor as the expansion variable. Note that an expansion around $z = 0$ is translated to an expansion around $a = 1$ when the scale factor is used as the expansion variable. The standard approach consists in taking the expansion center at $z = 0$ ($a = 1$). However, nothing prevents us from changing the expansion center to an arbitrary redshift or scale factor. By assuming that the Hubble parameter and the luminosity distance are analytical functions in the range $]\tilde{a} - \epsilon, \tilde{a} + \epsilon[$, where \tilde{a} is expansion center, we get

$$\begin{aligned} H(a) = & \tilde{H} \left\{ 1 + (1 + \tilde{q}) \left(1 - \frac{a}{\tilde{a}} \right) \right. \\ & + \frac{1}{2}(2 + 2\tilde{q} - \tilde{q}^2 + \tilde{j}) \left(1 - \frac{a}{\tilde{a}} \right)^2 \\ & - \frac{1}{6}(\tilde{s} - 3\tilde{j} + 3\tilde{q}^2 - 3\tilde{q}^3 - 6\tilde{q} + 4\tilde{q}\tilde{j} - 6) \left(1 - \frac{a}{\tilde{a}} \right)^3 \\ & + \frac{1}{24}[\tilde{l} + 7\tilde{q}\tilde{s} + 5\tilde{q}^2(5\tilde{j} - 3\tilde{q}^2) - 4\tilde{j}^2 \\ & - 4(\tilde{s} - 3\tilde{j} + 3\tilde{q}^2 - 3\tilde{q}^3 - 6\tilde{q} + 4\tilde{q}\tilde{j} - 6)] \\ & \left. \times \left(1 - \frac{a}{\tilde{a}} \right)^4 + \dots \right\} \end{aligned} \quad (6)$$

and

TABLE I: Constraints on H , q , j , and s at $z = 0$ obtained from H and d_L measurements for successive approximation orders of the expansions (6) and (7). The error bars correspond to 2σ ($\Delta\chi^2 = 4$) statistical uncertainty for a single parameter. The χ^2_{min} values shows that the relevant approximation order for both expansions is the 3rd.

Approximation order	H_0	q_0	j_0	s_0	l_0	χ^2_{min}	Observable
2nd	$73.9^{+4.8}_{-4.8}$	$-1.73^{+0.70}_{-0.64}$	$13.1^{+6.4}_{-5.8}$	-	-	15.53	Hubble parameter
3rd	$73.8^{+4.7}_{-4.7}$	$-0.92^{+1.49}_{-1.41}$	$-0.4^{+21.6}_{-18.4}$	$-45.0^{+263}_{-86.0}$	-	13.44	
4th	$72.9^{+4.7}_{-4.7}$	$0.16^{+3.04}_{-3.24}$	-23.4^{+77}_{-57}	-256.0^{+1256}_{-194}	1080^{+38020}_{-3580}	13.06	
3rd	$69.98^{+1.08}_{-1.08}$	$-0.51^{+0.38}_{-0.39}$	$-0.60^{+4.8}_{-3.9}$	-	-	562.19	Distance modulus
4th	$69.97^{+1.43}_{-1.41}$	$-0.50^{+0.86}_{-0.90}$	$-0.71^{+19.24}_{-14.43}$	$-18.8^{+321.2}_{-83.59}$	-	562.19	

$$\begin{aligned}
\frac{\tilde{H}d_L(a)}{c} &= \frac{1}{a} \left\{ \tilde{a} \frac{\tilde{H}\tilde{d}_L}{c} + \frac{1}{\tilde{a}} \left(1 - \frac{a}{\tilde{a}} \right) \left[1 + \frac{1}{2}(1 - \tilde{q}) \right. \right. \\
&\times \left(1 - \frac{a}{\tilde{a}} \right) + \frac{1}{6}(2 - 2\tilde{q} + 3\tilde{q}^2 - \tilde{j}) \left(1 - \frac{a}{\tilde{a}} \right)^2 \\
&+ \frac{1}{24}(\tilde{s} - 3\tilde{j} + 9\tilde{q}^2 - 15\tilde{q}^3 - 6\tilde{q} + 10\tilde{q}\tilde{j} + 6) \\
&\times \left(1 - \frac{a}{\tilde{a}} \right)^3 - \frac{1}{120}(\tilde{l} + 15\tilde{q}\tilde{s} + 105\tilde{q}^2\tilde{j} - 10\tilde{j}^2 \\
&- 105\tilde{q}^4 - 4\tilde{s} + 12\tilde{j} - 36\tilde{q}^2 + 60\tilde{q}^3 + 24\tilde{q} \\
&- 40\tilde{q}\tilde{j} - 24) \left(1 - \frac{a}{\tilde{a}} \right)^4 \left. \right\}, \quad (7)
\end{aligned}$$

where a tilde denotes a function evaluated at \tilde{a} . The main advantage of this procedure is that we can estimate the value of the cosmographic parameters at $z \neq 0$ and so, changing the expansion center, discover how these parameters evolve in a completely model-independent way. Note that $\tilde{d}_L = d_L(\tilde{a})$ is also a free parameter in our cosmographic analysis. Since $d_L = 0$ at $a = 1$, we can write \tilde{d}_L in terms of \tilde{H} , \tilde{q} , \tilde{j} and so on. Thus, by expanding H and d_L around an arbitrary scale factor \tilde{a} it is possible to obtain the cosmographic parameters as a function of a independent of the underlying cosmological model. Also, it is worth mentioning that the lower the value of ϵ the better the approximation that describes the real H and d_L functions.

III. OBSERVATIONAL CONSTRAINTS

A. Data

In order to constrain the cosmographic parameters we use separately the 580 SNe Ia distance measurements of the Union 2.1 compilation [26] and the 30 measurements of the Hubble parameter compiled in [27], plus the measurement of the Hubble constant $H_0 = 73.24 \pm 1.74 \text{ Km} \cdot \text{s}^{-1} \cdot \text{Mpc}^{-1}$ provided by [28]. The SNe Ia data are distributed in the redshift interval $0.015 \leq z \leq 1.414$ ($0.414 \leq a \leq 0.985$), corresponding to a maximum ϵ of ~ 0.571 , while the Hubble parameter data cover the redshift range $0 \leq z \leq 1.965$ ($0.337 \leq a \leq 1$), corresponding to a maximum ϵ of ~ 0.663 .

For SNe Ia data, the statistical analysis is performed using the distance modulus definition:

$$\begin{aligned}
\mu(z|\{\theta_i\}) &= 5 \log_{10} d_L(z|\{\theta_i\}) + 25 \\
&= 5 \log_{10} \left(\frac{\tilde{H}d_L}{c} \right) - 5 \log_{10} \left(\frac{\tilde{h}}{3} \right) + 40, \quad (8)
\end{aligned}$$

where $\{\theta_i\} = \{\tilde{H}, \tilde{q}, \tilde{j}, \dots\}$ is the set of parameters to be fitted and $\tilde{h} = \tilde{H}/(100 \text{ Km} \cdot \text{s}^{-1} \cdot \text{Mpc}^{-1})$. The best fit parameters are obtained by minimizing the quantity

$$\chi^2_{\text{SN}}(\{\theta_i\}) = \sum_{i=1}^{580} \frac{[\mu(z|\{\theta_i\}) - \mu^{\text{obs}}(z_i)]^2}{\sigma_{\mu,i}^2}, \quad (9)$$

where $\mu^{\text{obs}}(z_i)$ is the observed value of the distance modulus at redshift z_i and $\sigma_{\mu,i}^2$ is the error of $\mu^{\text{obs}}(z_i)$.

For the Hubble parameter data, the best fit parameters are obtained by minimizing the quantity

$$\chi^2_H(\{\theta_i\}) = \sum_{i=1}^{31} \frac{[H(z|\{\theta_i\}) - H^{\text{obs}}(z_i)]^2}{\sigma_{H,i}^2}, \quad (10)$$

where $H^{\text{obs}}(z_i)$ is the observed value of the Hubble parameter at z_i and $\sigma_{H,i}^2$ is the error associated with the $H^{\text{obs}}(z_i)$ measurement.

B. F-test

In order to decide the order in which the series should be stopped, we perform the so-called F -test, defined as

$$F_{kl} = \frac{\chi_k^2 - \chi_l^2}{n_l - n_k} \frac{\chi_l^2}{N - n_l}, \quad (11)$$

where χ_i^2 and n_i are, respectively, the minimum chi-squared function and the number of parameters of the i th model and N is the number of data points. This test compares two models, identifying the one that provides the best fit to the data, with the null hypothesis implying the correctness of the first model. In the following we compare successive truncations of the Taylor series (6) and (7) to decide the number of parameters that we need to take into account in our analysis. Table I displays the constraints on the cosmographic parameters at

the present time for successive approximations of H and d_L . It is easy to see that for both expansions the last relevant term is the third, $F_{34} \approx 0.2$ for H and $F_{34} = 0$ for d_L . However, the third order approximation of H contains four parameters while the third order approximation of d_L contains three parameters. This implies that if we want to compare the results obtained from H data with the results obtained from SNe Ia data or combine the two data sets we must include one term beyond than necessary in the d_L series approximation. In what follows we take the third order approximation of H and the fourth order approximation of d_L and compare the constraints on H , q , j , and s obtained from $H(z)$ and SNe Ia data.

C. Results

The evolution of the cosmographic parameters H , q , j and s is obtained following the algorithm:

1. fix the expansion center $\tilde{a}_i = (1 + \tilde{z}_i)^{-1}$ in eqs. (6) and (7);
2. perform the statistical analysis with H and SNe Ia data to constrain H , q , j and s at \tilde{z}_i ;
3. set $\tilde{z}_{i+1} = \tilde{z}_i + \Delta\tilde{z}$ and repeat the previous step to constrain H , q , j and s at \tilde{z}_{i+1} .

Here we take a step of $\Delta\tilde{z} = 0.1$ and cover the interval $0 \leq \tilde{z}_i \leq 1.4$ for both data sets used in our analysis.

Tables II and III contain, respectively, the results obtained from H and SNe Ia data. The errors correspond to a 2σ ($\Delta\chi^2 = 4$) confidence interval for each parameter. In both cases the reduced chi-square values ($\chi^2_{\nu} = \chi^2_{min}/\text{NDoF}$) remain unchanged when the expansion center is shifted.

A graphical representation of the results contained in Tables (II) and (III) is given in Figs. 1 and 2. Figure 1 shows the constraints on H (left panel) and q (right panel) and Figure 2 shows the constraints on j (top panel) and s (bottom panel) at 15 points equally spaced in the redshift range $0 \leq z \leq 1.4$. The blue boxes stand for 2σ confidence intervals obtained from H data while the orange boxes stand for 2σ confidence intervals obtained from SNe Ia data. The gray region in the q plot, the dashed line in the j plots and the gray region in the s plots correspond, respectively, to the Λ CDM bounds:

$$\begin{aligned} q(a) &= -1 + \frac{3H_0^2\Omega_{m,0}}{2H^2a^3} > -1, \\ j(a) &= 1 \quad \text{and} \\ s(a) &= 1 - \frac{9H_0^2\Omega_{m,0}}{2H^2a^3} < 1, \end{aligned} \quad (12)$$

where $\Omega_{m,0}$ is matter density parameter at the present time.

For $z < 1$ the constraints on H obtained from SNe Ia data are tighter than the constraints obtained from H

TABLE II: Estimates of H , q , j , and s as function of the redshift obtained from H measurements for the 3rd order approximation of the Hubble parameter (6). The errors correspond to 2σ ($\Delta\chi^2 = 4$) statistical uncertainty for each parameter. $\chi^2_{min} = 13.44$ for all redshifts considered.

z	H	q	j	s
0.0	$73.8^{+4.7}_{-4.7}$	$-0.92^{+1.49}_{-1.41}$	$-0.40^{+21.6}_{-18.4}$	$-45.0^{+263}_{-86.0}$
0.1	$74.3^{+5.0}_{-5.0}$	$-0.87^{+0.43}_{-0.47}$	$2.50^{+9.80}_{-8.70}$	$-15.0^{+110}_{-85.0}$
0.2	$75.8^{+5.2}_{-5.2}$	$-0.66^{+0.42}_{-0.49}$	$3.21^{+3.99}_{-3.41}$	$-2.99^{+45.0}_{-47.0}$
0.3	$78.8^{+5.0}_{-4.9}$	$-0.39^{+0.47}_{-0.48}$	$3.16^{+1.94}_{-1.66}$	$1.50^{+21.5}_{-22.5}$
0.4	$83.1^{+5.6}_{-5.6}$	$-0.16^{+0.41}_{-0.46}$	$2.76^{+2.16}_{-1.80}$	$2.80^{+12.8}_{-10.0}$
0.5	$88.6^{+6.5}_{-6.8}$	$0.01^{+0.32}_{-0.32}$	$2.25^{+2.43}_{-2.08}$	$3.30^{+15.5}_{-5.80}$
0.6	$94.5^{+8.2}_{-7.3}$	$0.14^{+0.24}_{-0.26}$	$1.70^{+2.46}_{-2.10}$	$3.90^{+5.9}_{-5.10}$
0.7	$102.0^{+8.4}_{-8.4}$	$0.21^{+0.24}_{-0.23}$	$1.25^{+2.35}_{-2.05}$	$4.30^{+12.4}_{-4.70}$
0.8	$109.6^{+8.7}_{-8.9}$	$0.25^{+0.28}_{-0.27}$	$0.80^{+2.20}_{-1.85}$	$4.70^{+2.30}_{-4.00}$
0.9	$117.1^{+9.1}_{-9.0}$	$0.27^{+0.32}_{-0.32}$	$0.50^{+1.92}_{-1.56}$	$4.90^{+1.75}_{-2.85}$
1.0	$125.0^{+9.3}_{-9.4}$	$0.26^{+0.35}_{-0.35}$	$0.17^{+1.71}_{-1.41}$	$4.98^{+1.07}_{-2.39}$
1.1	$132.9^{+10.0}_{-10.0}$	$0.25^{+0.38}_{-0.37}$	$-0.06^{+1.45}_{-1.21}$	$4.95^{+1.01}_{-3.11}$
1.2	$140.7^{+11.2}_{-11.1}$	$0.22^{+0.40}_{-0.38}$	$-0.27^{+1.23}_{-0.99}$	$4.76^{+1.24}_{-3.60}$
1.3	$148.5^{+12.8}_{-12.7}$	$0.20^{+0.38}_{-0.44}$	$-0.42^{+1.01}_{-0.81}$	$4.59^{+1.50}_{-3.97}$
1.4	$156.3^{+14.6}_{-14.9}$	$0.16^{+0.38}_{-0.43}$	$-0.58^{+0.85}_{-0.62}$	$4.25^{+1.93}_{-4.08}$

TABLE III: Estimates of H , q , j , and s as function of the redshift obtained from Union 2.1 SNe Ia sample for the 4th order approximation of d_L (7). The errors correspond to a 2σ ($\Delta\chi^2 = 4$) statistical uncertainty for each parameter. $\chi^2_{\nu} = \chi^2_{min}/\text{NDoF} = 0.976$ for all redshifts considered.

z	H	q	j	s
0.0	$69.97^{+1.43}_{-1.41}$	$-0.50^{+0.86}_{-0.90}$	$-0.71^{+19.2}_{-14.4}$	$-18.8^{+321}_{-83.6}$
0.1	$73.32^{+1.26}_{-1.30}$	$-0.50^{+0.14}_{-0.16}$	$0.51^{+4.83}_{-4.86}$	$-8.40^{+79.2}_{-90.0}$
0.2	$76.76^{+1.20}_{-1.20}$	$-0.42^{+0.25}_{-0.25}$	$1.04^{+1.24}_{-1.24}$	$-3.25^{+30.7}_{-32.3}$
0.3	$80.66^{+2.10}_{-1.96}$	$-0.33^{+0.20}_{-0.19}$	$1.25^{+1.93}_{-2.09}$	$-2.40^{+14.4}_{-8.40}$
0.4	$85.08^{+2.73}_{-2.52}$	$-0.23^{+0.16}_{-0.16}$	$1.25^{+2.20}_{-2.37}$	$-1.70^{+5.50}_{-4.90}$
0.5	$90.10^{+2.90}_{-2.80}$	$-0.14^{+0.24}_{-0.25}$	$1.19^{+2.31}_{-2.15}$	$-1.75^{+2.20}_{-7.48}$
0.6	$95.50^{+3.50}_{-3.30}$	$-0.04^{+0.33}_{-0.36}$	$1.29^{+2.31}_{-1.93}$	$-2.25^{+1.35}_{-10.8}$
0.7	$101.17^{+5.28}_{-4.51}$	$-0.02^{+0.46}_{-0.42}$	$1.21^{+2.66}_{-1.53}$	$-2.53^{+0.10}_{-15.0}$
0.8	$107.20^{+8.10}_{-6.30}$	$0.06^{+0.55}_{-0.45}$	$1.13^{+2.85}_{-1.15}$	$-2.75^{+0.75}_{-17.5}$
0.9	$115.04^{+10.81}_{-10.58}$	$0.18^{+0.57}_{-0.55}$	$1.33^{+2.88}_{-1.16}$	$-3.76^{+1.61}_{-19.8}$
1.0	$122.08^{+15.36}_{-13.76}$	$0.21^{+0.64}_{-0.55}$	$1.28^{+3.29}_{-0.94}$	$-3.90^{+1.70}_{-23.5}$
1.1	$129.90^{+20.40}_{-17.10}$	$0.27^{+0.62}_{-0.55}$	$1.37^{+3.08}_{-0.87}$	$-4.50^{+2.25}_{-22.3}$
1.2	$136.60^{+25.87}_{-20.09}$	$0.29^{+0.73}_{-0.54}$	$1.32^{+3.59}_{-0.73}$	$-4.50^{+2.17}_{-26.9}$
1.3	$146.50^{+25.97}_{-23.85}$	$0.36^{+0.63}_{-0.54}$	$1.45^{+3.03}_{-0.78}$	$-5.30^{+3.03}_{-22.1}$
1.4	$154.90^{+34.45}_{-25.35}$	$0.38^{+0.71}_{-0.50}$	$1.44^{+3.57}_{-0.71}$	$-5.40^{+3.07}_{-27.0}$

measurements, reversing the roles for $z \geq 1$. A similar behavior is observed for q , with SNe Ia providing tighter constraints for $z \leq 0.5$. For j the constraints obtained from $H(z)$ data are tighter than the constraints provided by the SNe Ia data for $z \geq 1$, while the constraints on s obtained from H data are tighter than those obtained from SNe Ia data for $z \geq 0.8$. The constraints on j obtained from H data begin to depart from those from

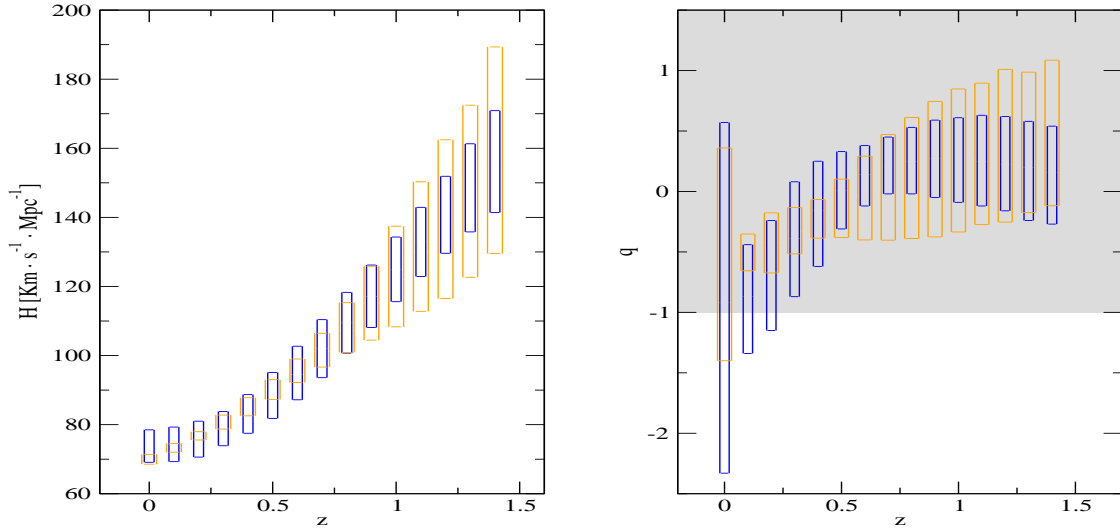


FIG. 1: Redshift evolution of H (left panel) and q (right panel). The blue boxes corresponds to the constraints obtained from H data while the orange boxes corresponds to the constraints obtained from SNe Ia data. The gray region represents the region allowed for the Λ CDM model ($q > -1$).

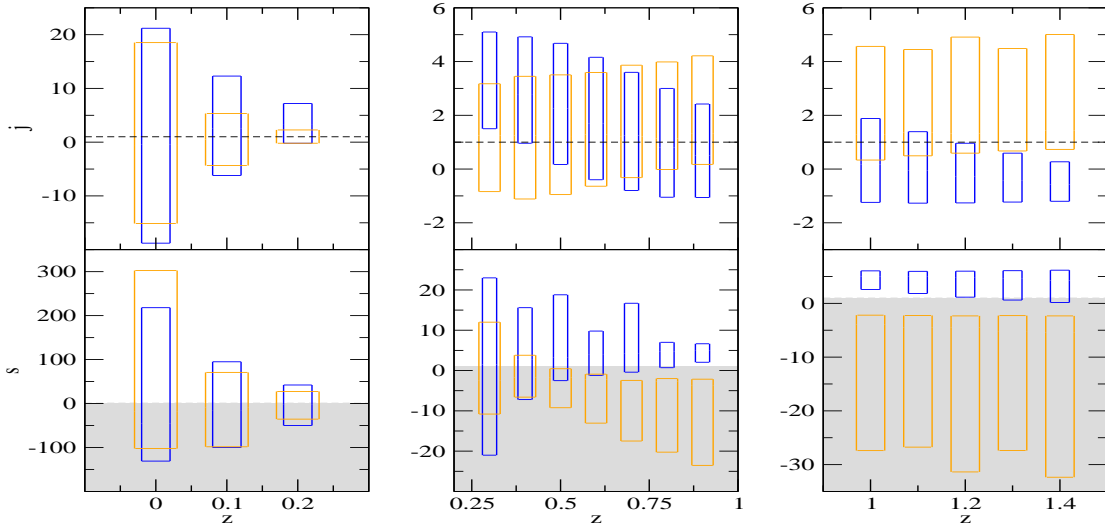


FIG. 2: Redshift evolution of j (top panels) and s (bottom panels). The blue boxes corresponds to the constraints obtained from H data while the orange boxes corresponds to the constraints obtained from SNe Ia data. The dashed line represents the Λ CDM model ($j = 1$). The gray region represents the region allowed for the Λ CDM model ($s < 1$).

SN e Ia data for $z > 0.8$, going to negative values. For the snap, the difference between the results obtained from SNe Ia and $H(z)$ data begins at $z > 0.5$.

As we can see, the results obtained from SNe Ia data are in agreement with the Λ CDM bounds, but the results obtained from H data are not. These results indicate a discrepancy between the H and SNe Ia data sets. Such a discrepancy cannot be seen when we restrict our analysis

to the neighborhood of $z = 0$. At $z = 0$, the constraints on the parameters j and s are completely without statistical significance. Therefore, the standard cosmographic approach, which consists in expanding the Taylor series of H and d_L around $z = 0$, does not seem a useful tool for testing models designed to explain the cosmic acceleration. This result is in agreement with the findings of [29]. However, since their results remain valid regardless

of the underlying cosmology, performing the series expansion around an arbitrary $\tilde{a} \neq 1$ cosmography can still be an efficient way to rule out cosmological models. For instance, a single value of $j \neq 1$ for some $z \neq 0$ should be considered as evidence against the Λ CDM model.

It is important to note that, at $z = 0$, the results of our analysis do not exclude a decelerated Universe, $q_0 > 0$. However, it is an observational fact that, at the present time, the Universe is expanding at an accelerated rate [1, 2], i.e., $q_0 < 0$. So, how can we explain such a result? For SNe Ia data, this result can be explained by the fact that we are working with more terms in the d_L expansion than necessary. When the expansion of d_L is truncated at the most statistically significant term, we have $q_0 < 0$ at 2σ (see Table I). Since, for H data, we are already using the most relevant approximation, we suspect that this result may be due the low number of H measurements or to the lack of precision of these measurements, or both.

Also note that, at least for the approximations used here, values of $q < 0$ are allowed in the entire redshift interval considered, i. e., both SNe Ia and H data sets are compatible with an early time accelerated Universe. For SNe Ia, values of $q > 0$ are allowed for $z \geq 0.5$, indicating that the transition between the decelerated to accelerated phases should occur for redshifts greater than 0.5. In turn, for H data, positive values of q are allowed for $z \geq 0.3$ showing that in this case the transition redshift, z_t , is greater than 0.3.

Also, we observe that from $z \geq 0.6$ onwards the constraints on the snap obtained from SNe Ia data begin to become incompatible with the constraints coming from H data. This means that we cannot combine the two data sets to reconstruct the time-dependence of the cosmographic parameters.

Finally, it should be mentioned that, even working with more parameters than necessary (which can be seen as a conservative analysis), the constraints obtained from SNe Ia data barely touch the Λ CDM diagnostic line $j = 1$. That is, although compatible with the results, the Λ CDM is not the model most consistent with the data.

IV. FINAL REMARKS

In this paper we have used the cosmographic approach to constrain the Hubble (H), deceleration (q), jerk (j) and snap (s) parameters at $z \neq 0$ from SNe Ia and Hubble parameter data. These constraints are obtained from data by changing the expansion center of the H and d_L

Taylor series at small intervals. Such simple implementation allows us to map the time evolution of the cosmographic parameters without assuming a specific gravity model or making assumptions about the sources. This approach can be a useful tool to decide between modified gravity or dark energy models designed to explain the current accelerated expansion of the Universe. For instance, for the main candidate used to explain the present cosmic acceleration, the Λ CDM model, $j = 1$. In the usual approach, where the expansion center is fixed at $z = 0$, evidence against the Λ CDM model is possible only if we find $j_0 \neq 1$ with some statistical significance. However, many cosmographic analyses performed with multiple data sets have shown that the constraints on j_0 are too weak and do not allow us to decide either for or against Λ CDM (or many other competing models). On the other hand, in the method used in this paper, it is enough to find a single value of $j \neq 1$ with some statistical significance to rule out the Λ CDM model.

We show that, although it is not the favored model, the Λ CDM model is in agreement with the constraints obtained from the SNe Ia data. In turn, the results obtained from $H(z)$ data do not accommodate the Λ CDM model.

These conflicting results may indicate a tension between SNe Ia and $H(z)$ data, which is masked at $z = 0$. Such a discrepancy indicates that we cannot combine these two data sets to reconstruct the time evolution of the kinematic parameters. In fact, the Taylor series of H and d_L cannot be treated on equal footing since we need to include more terms than necessary in the d_L approximation to make the comparison possible. Therefore, the constraints on the cosmographic parameters obtained from SNe Ia data are weaker than they should be. Even so, the 2σ bounds do not overlap. If we look at the results of $H(z)$ data separately, we will conclude that the Λ CDM model is excluded. However we cannot make such an extreme statement given the small number of H measurements and large uncertainties involving these data. We hope that future analyses with more accurate H data can help us to clarify this problem.

Acknowledgments

CRF acknowledges the financial support from Coordenação de Aperfeiçoamento de Pessoal de Nível Superior (CAPES). The authors acknowledge Thomas Dumelow and Jailson Alcaniz for useful comments.

-
- [1] Riess A. et al., 1998, *Astron.J.*, **116**, 1009
 - [2] Perlmutter S. et al., 1999, *Astrophys.J.*, **517**, 565
 - [3] Padmanabhan T., 2003, *Phys. Rept.*, **380**, 235
 - [4] Weinberg S., 1989, *Rev. Mod. Phys.*, **61**, 1
 - [5] Nojiri S. and Odintsov S. D., 2003, *Phys. Lett. B* **576**, 5
 - [6] Amendola L., Polarski D. and Tsujikawa S., 2007, *Phys.*

- Rev. Lett.* **98**, 131302
- [7] Capozziello S. and Felice A., 2008, *JCAP* **0808**, 016
- [8] Randall L. and Sundrum R., 1999, *Phys. Rev. Lett.* **83**, 3370
- [9] Dvali G., Gabadadze G. and Porrati M., 2000, *Phys. Lett. B* **485**, 208

- [10] Deffayet C., 2001, Phys. Lett. B **502**, 199
- [11] Dick R., 2001, Class. Quant. Grav. **18**, R1
- [12] Wetterich C., 1988, Nucl. Phys. B **302**, 668
- [13] Caldwell R., 2002, Phys. Lett. B **545**, 23
- [14] Setare M. R. and Saridakis E. N., 2008, JCAP **0809**, 026
- [15] Chiba T. and Nakamura T., 1998, Prog. Theor. Phys., **100**, 1077
- [16] Visser M., Class. Quant. Grav., 2004, **21**, 2603.
- [17] Visser M., Gen. Rel. Grav., 2004, **37**, 1541.
- [18] Rapetti D. et al., 2007, MNRAS, **375**, 1510
- [19] Turner M. S. and Riess A. G., 2002, Astrophys.J., **569**, 18
- [20] Alam L. et al., 2003, MNRAS **344**, 1057
- [21] Cattöen C. and Visser M., 2007, Class. Quant. Grav., 24, 5985
- [22] Cattöen C. and Visser M., 2007, gr-qc/0703122
- [23] Barboza Jr. E. M. and Carvalho F. C., 2012, Phys. Lett. B, 715, 19
- [24] Vitagliano V. Xia J.-Q., Liberati S. and Viel M., 2010, JCAP, 1003, 005
- [25] Ade P. A. R. et al.: Planck Collaboration, 2015, A & A **594**, A13
- [26] Suzuki N. et al.: The supernova Cosmology Project, Astrophys. J., 2012, **746**, 85.
- [27] Moresco M., et al., 2016, JCAP, 0516, 014
- [28] Riess A. et al., 2016, Astrophys. J., **826**, 56
- [29] Busti V. C. et al., 2015, Phys. Rev D, **92**, 123512